Role of the interface for the electronic structure of Si quantum dots

Dirk König,* James Rudd, Martin A. Green, and Gavin Conibeer
ARC Photovoltaics Centre of Excellence, The University of New South Wales, Sydney, NSW 2052, Australia
(Received 2 October 2007; revised manuscript received 22 April 2008; published 31 July 2008)

Approximants consisting of 1–165 Si atoms with complete fluorine (F), hydroxyl (OH), amino (NH_2), methyl (CH_3), and hydrogen (H) termination were investigated by density-functional-Hartree-Fock (DF-HF) ground-state (GS) calculations within the B3LYP hybride functional formalism using a 6–31G(d) Gaussian type molecular-orbital (MO) basis set. With increasing polarity of the Si interface bonds, the highest occupied MO (HOMO)-lowest unoccupied MO (LUMO)-gaps depend less on quantum confinement but more on the nature of the interface. The HOMO and LUMO positions are a function of the anion/functional group intended to model different dielectric matrices hosting the Si quantum dot (QD). We discuss the influence of the Si interface bond termination on charge transfer and local breakdown of the MO symmetry. Relating these observations to the ratio of interface anions to Si core atoms, we estimate a size range below which the electronic structure of Si QDs is determined exclusively by the nature of the interface bonds. For Si cores consisting of $\geq$10 Si atoms, the interface governs the electronic structure with quantum confinement competing for covalent and weak polar interface terminations or being only a secondary effect for strong polar interface terminations. We estimate that the interface has a major impact on the electronic structure of Si QDs in Si_3N_4, SiO_2, or fluorides to a Si core size of ca. 1330 atoms.

DOI: 10.1103/PhysRevB.78.035339 PACS number(s): 73.22.−f, 73.20.−r, 61.50.Ah, 71.15.Ap

I. INTRODUCTION

In the past two decades there has been a rising interest in quantum dot (QD) arrays and super lattices (SLs). They have the potential to serve as memory devices of extreme packing density[1] and eventually as smallest components of a quantum computer.[2] Their optoelectronic properties make them predestined for light emitting devices with the QD laser being potentially of the most spectacular advances in this field.[3,4]

Silicon (Si) QD-SLs as highly absorbing ultrathin active layers in a so-called third generation photovoltaic (PV) solar cell[5–7] present an application which emerged over the last decade. This concept is currently under intense theoretical and experimental studies.[8,9] The conceptual use of QDs in PV covers a wide range from an active PV layer with the benefit of a tunable band gap[5,10] to energy selective contacts[11,12] at hot carrier absorbers.[13] Quantum structures in a PV cell have shown to increase its short circuit current significantly.[14,15]

There is a current debate concerning whether the electronic structure of Si QDs are defined by either quantum confinement[16–21] or by their interface termination. In recent years it emerged that the Si QD interface with its surrounding dielectric matrix plays a decisive role in determining the optical gap and the optical activity of the Si QD on both experimental[22–27] and theoretical grounds as below.

Several research groups report on the influence of O double and bridge bonds terminating the Si surface of otherwise H terminated Si approximants,[28–31] occasionally with partial oxidation of the Si core.[32] Few publications exist on approximants consisting of an Si core in a silicon dioxide (SiO_2) shell.[31,33,34]

Si QDs in silicon nitride (Si_3N_4) were investigated by photo luminescence (PL) and shown to emit in the range of 640–720 nm for QD sizes of $d_{QD}=2-5$ nm.[35] The electronic structure of approximants consisting of an Si core terminated with H and very few NH_2 and —NH— bride bonds was reported together with PL signals in the range of 880 nm.[36] These emissions were assigned to the interface Si/Si_3N_4 or to defects in the Si rich Si_3N_4.

Terminating periodic approximants consisting of Si cores with alkyl (C_nH_{2n+1}) groups instead of H showed little impact on the optical gap of $Si_x(C_nH_{2n+1})_y$ approximants, but shifted the HOMO and LUMO significantly to lower binding energies.[37] This was attributed to repulsive Coulomb forces between alkyl groups and shown to reach an asymptotic limit for longer alkyl chains.

In this paper we describe the ground-state (GS) electronic structure of Si QDs surrounded by a dielectric as in an annealed Si rich SiO_2 (SRO) layer.[38,39] We perform a systematic analysis of Si core approximants by nonperiodic spatial space density-functional-Hartree-Fock (DF-HF) computations of Si approximants comprising 1–165 Si atoms corresponding to a spherical QD diameter of $d_{QD}=3.4-18.5$ Å. *All* surface bonds were terminated by the anions of the dielectric which were saturated with H as required, resulting in F, OH, NH_2, CH_3, and H terminations of the Si cores.

Section II describes the spatial structure of the approximants and gives an overview of the computational method used. In Sec. III we present the results of the DF-HF computations and discuss the impact of the interface on the electronic structure of the approximants in terms of optimized geometries, quantum chemical parameters, geometrical constraints, and interface charge transfer. Section IV summarizes the results.

II. COMPUTATION DETAILS

A. Structure of approximants and energetics

All approximants consist of an Si core fully terminated with functional groups emulating the respective dielectric in

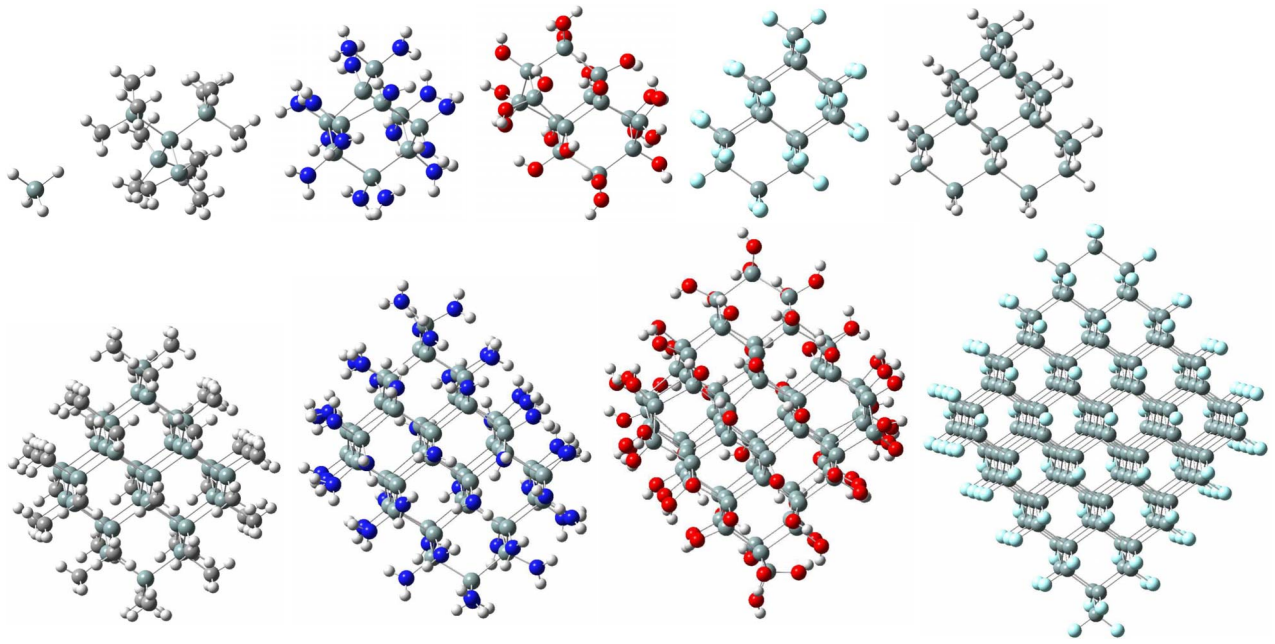

FIG. 1. (Color online) Optimized approximants (left to right; top to bottom): SiH_4, $Si_5(CH_3)_{12}$, $Si_{10}(NH_2)_{16}$, $Si_{14}(OH)_{20}$, $Si_{18}F_{24}$, $Si_{26}H_{32}$; $Si_{35}(CH_3)_{36}$, $Si_{53}(NH_2)_{48}$, $Si_{84}(OH)_{64}$, $Si_{165}F_{100}$. All interface terminations were realized for Si core sizes of up to 165 Si atoms apart from $Si_{165}(OH)_{100}$.

which the Si QDs are embedded: Fluorine (F) accounts for metal fluorides, hydroxyl groups (OH) emulate SiO_2, amino groups (NH_2) represent Si_3N_4, and methyl groups (CH_3) establish the link to SiC. In addition, H and F are bond terminations encountered on Si QDs prepared from silane (SiH_4) in a microwave plasma[26,27] or serve as a model system for Si QDs in an ionic dielectric matrix, respectively. This method serves as an approximation of the Si core termination in analogy to first next neighbor (1-nn) tight-binding (TB) methods, while keeping the required computation power affordable.

The examined approximants with *complete* interface terminations by the respective functional group/anion ($X[Si_xX_y]$=F, OH, NH_2, CH_3, and H) are shown in Fig. 1 after optimization with one type of interface bond termination per Si core specimen. Possibly all surfaces the Si cores have a $\langle 111 \rangle$ orientation, accounting for the lowest surface energy and the associated maximum crystal growth along this plane.[40,41] In total, 49 Si cores with functional group/anion termination were investigated.

B. Algorithm and software

As computation software we used the software package GAUSSIAN03, revision D.01.[42] For the visualization of approximants, spatial MO, and charge-density distributions, we used GAUSSVIEW 3.09.[43] Approximants where optimized with the HF method using a 3–21 G* Gaussian type MO basis until the forces acting on all atoms were below 0.012 eV/Å and the RMS force was below 0.008 eV/Å. The electronic structure was then calculated using the three-parameter B3LYP hybride functional of Becke[44] and Lee *et al.*[45] together with a Gaussian type 6–31(d) MO basis set. This combination of optimization and electronic structure computation is reasonably accurate while not requiring excessive computation power.[46] Its accuracy matches an optimization and single point energy calculation with a B3LYP/6–31G(d) functional/MO basis set throughout as verified by the G2 standard molecule set,[46,47] cf. Table I. For a critical discussion about the accuracy regarding electronic structure values, the reader is referred to Ref. 48 of this article.

On H-terminated approximants up to $Si_{35}H_{36}$, additional electronic structure calculations were carried out with an extended high accuracy basis set [6–311+G(2*d*,*p*)]. The standard deviation of the HOMO-LUMO gap to the 6–31G(d) basis set was 0.12 eV.

TABLE I. Error statistics of experimental thermochemical data of the G2 standard molecule set (Refs. 46 and 47). Algorithms used for optimization (opt) and GS single point energy (spE) in our work are shown along with a B3LYP/6–31G(d) DF/MO basis set used throughout. All values are given in kJ/mol.

opt, spE	MAD[a]	stdDev[b]	Largest errors pos	neg
HF/3–21G*, B3LYP/6–31G(d)	33.5	39.4	39.4	−227.1
HF/3–21G*, B3LYP/6–311+G(2d,p)	13.4	12.6	57.8	−88.82
B3LYP/6–31G(d), B3LYP/6–31G(d)	33.1	39.8	51.1	−227.1

[a]Mean absolute deviation.
[b]Standard deviation.

III. RESULTS AND DISCUSSION

A. Spatial structure and approximation of dielectric by functional groups

In Fig. 1 it can be seen that the Si approximants terminated with OH or NH_2 groups show a significant deviation of some atomic positions from the bulk Si lattice after optimization. This is due to the polar nature of the Si interface bonds in compound with the altered MO geometry invoked by the anion. The former leads to electrostatic forces between the anions and the H atoms of the functional groups. The latter causes the cubic symmetry of the Si core to be broken locally. Both result in an altered local geometry. CH_3-terminated Si approximants do not show any significant geometrical deviation due to the weak polar bond Si-C. Si cores terminated with H have covalent Si interface bonds with H possessing a spherical MO symmetry which does not alter the Si core symmetry. In a similar way, F-terminated Si approximants do not show any noticeable deviation from the cubic Si symmetry although the bond Si-F is highly polar. The negatively charged F atoms have a cubic orbital symmetry ($2s^2 2p^6 \rightarrow$ Ne).

The spatial deviations are a partial consequence of the missing dielectric matrix which would impose spatial constraints on the anions bound to the Si core. However, the breaking of the MO symmetry of the Si core due to O and N atoms is still present if the Si core is embedded into a dielectric matrix.

Using functional groups for emulating the respective dielectric works well as a first-order approximation. This can be seen at the charge transfer from the H ligands to the respective interface anions which is constant over the size range of the Si cores, while the charge transfer from the Si core to the interface anions is changing, cf. Fig. 6. Recent calculations of a Si_{10} core embedded into 1.5 monolayers (MLs) of α-SiO_2 showed a change in the HOMO-LUMO gap of 0.05 eV referring to the $Si_{10}(OH)_{16}$ approximant, accounting for a relative change of 1.6%. This shift can be expected to decrease for an increasing Si core size, cf. Sec. III D. There is no change in energies of the MOs localized within the Si_{10} core when going from 1.5 to 2 ML α-SiO_2.[49] For the low band-gap dielectric SiC, the emulation by CH_3 groups at the Si core interface neglects the leakage of the MO wave functions into SiC which counteracts quantum confinement. As a consequence, the UMO energies would be lowered while the OMO energies would rise. Extrapolating the results of CH_3-terminated approximants, this limit would be reached for Si core diameters of $d_{QD} \approx 30$ Å. For the aim of this work the missing SiC matrix is an advantage as the impact of the actual interface can be examined.

B. HOMO, LUMO, and gap energies

Figure 2 shows the HOMO-LUMO gap of Si approximants with F, OH, NH_2, CH_3, and H termination, cf. Fig. 1. H-terminated Si approximants serve as a reference due to the covalent bond Si-H, cf. Sec. III A.

The HOMO-LUMO gap of $Si_{35}H_{36}$ and $Si_{35}(OH)_{36}$ approximants of Zhou *et al.*[33] who used the same MO sets are in good agreement with our results. Garoufalis and Zdetsis[50]

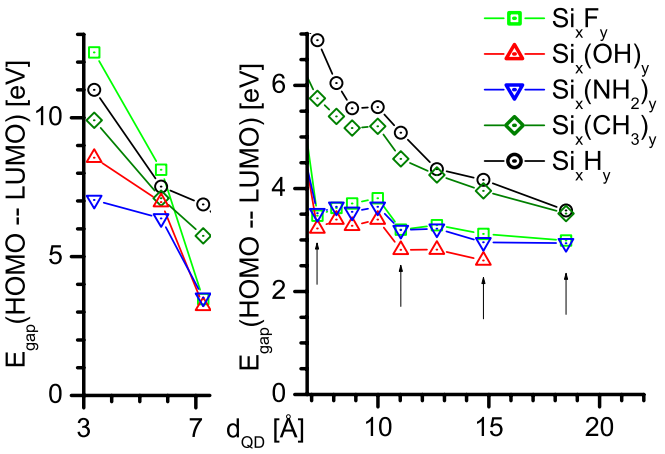

FIG. 2. (Color online) HOMO-LUMO gap as a function of the QD diameter for Si QDs with different interface terminations. For clarity, the graph is split into two subgraphs with different energy scale. The points for the $Si_{10}X_{16}$ approximants (d_{QD}=7.3 Å) are shown in both graphs. Arrows indicate the high-symmetry approximants $Si_{10}X_{16}$, $Si_{35}X_{36}$, $Si_{84}X_{64}$, and $Si_{165}X_{100}$ (see text).

obtained a HOMO-LUMO gap of 2.6 eV which is still in good agreement with our results, cf. Ref. 48. A valuable discussion of various modifications of O bonding (bridge and double bonded O) to the otherwise H-terminated Si core and its impact on the electronic structure can be found in Ref. 50, though the authors did not calculate approximants with otherwise complete OH termination as would be more appropriate for Si QDs embedded into SiO_2.

Recently, Hadjisavvas and Kelires[51] used a GGA algorithm with a Perdew-Wang exchange-correlation functional for calculating Si_{13} and Si_{40} cores in amorphous SiO_2 as derived from molecular-dynamic calculations. By repeating the GGA calculations with a purely H-terminated frozen Si core, it was reported that the atomic displacement within the Si core is the major reason for a significant decrease of the band gap. Their band gap of a Si_{40} core is 1.3 eV below the HOMO-LUMO gap of the $Si_{35}(OH)_{36}$ in this work, see Ref. 48. We also notice that the band gap of SiO_2 of 5 eV obtained by Hadjisavvas and Kelires is clearly too small. For an α-quartz approximant ($Si_{29}O_{76}H_{36}$) calculated with the same formalism used in this work, we obtained a HOMO-LUMO gap of 7.6 eV. This is still an underestimation of the experimental SiO_2 band gap which is 8.8–9 eV.[52,53] While the impact of stress on the electronic structure of approximants due to the change in interatomic distances and orbital symmetries is certainly important, we cannot confirm this argument by our results. Indeed, the optimized approximants in Fig. 1 show local deviations from the cubic symmetry of the unrelaxed Si core for the OH-terminated and - to a lesser degree - NH_2-terminated Si cores. In contrast, the F-terminated Si cores do not show a visible deviation of the Si core from its cubic symmetry. If stress would dominate over the chemistry at the interface, the HOMO-LUMO gaps of NH_2-, OH-, and F-terminated Si cores should have a major difference in the HOMO-LUMO gap as a function of the Si core size. While this is not the case, small deviations from the energetic trend can be observed when

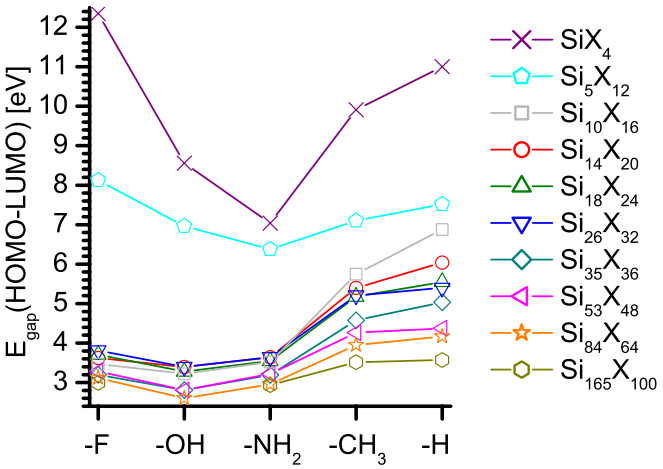

FIG. 3. (Color online) HOMO-LUMO gaps of Si_xX_y approximants arranged after increasing ionicity (right to left) of the functional group terminating the outer Si bonds.

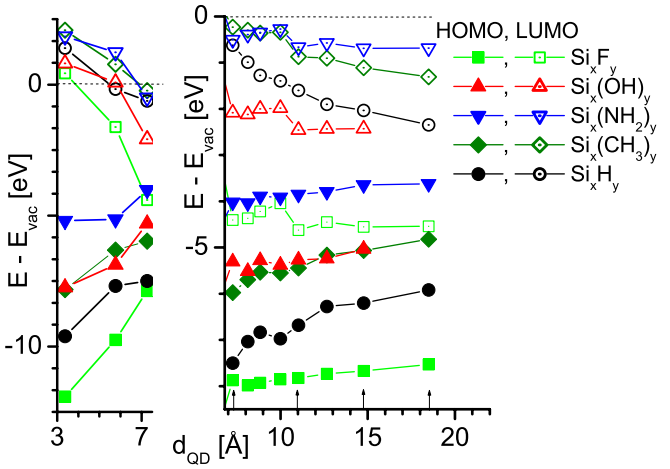

FIG. 4. (Color online) HOMO and LUMO energies as a function of the QD diameter for Si QDs with different interface terminations. For clarity, the graph is split into two subgraphs with different energy scale. The points for the $Si_{10}X_{16}$ approximants (d_{QD} =7.3 Å) are shown in both graphs. Arrows indicate the high-symmetry approximants (see also Fig. 2).

comparing the F- and NH_2-terminated Si cores, cf. Fig. 2 and the numerical results in the Ref. 48. However, interface anions can cause a local change in the MO symmetry by their hybrid AOs deviating from Si, leading to a Jahn-Teller distortion.[54] This has an influence on the DOS and the HOMO-LUMO gap, see Sec. III C. A deconvolution of both phenomena regarding the impact on the HOMO-LUMO gap is another complex issue and beyond the scope of this work.

For $Si_x(CH_3)_y$ approximants, we get a larger HOMO-LUMO gap than Reboredo and Galli[37] who used a PBE functional.[55] We did not find further literature on *ab initio* data for comparing our results of completely F- and NH_2-terminated approximants. However, PL characterization showed that ultrasmall Si QDs embedded in Si_3N_4 have a band gap which is 0.6 eV larger compared to Si QDs of the same size embedded in SiO_2.[56] Our calculations are consistent with this experimental result.

Figure 2 shows that the HOMO-LUMO gap and its gradient $\Delta E(\text{HOMO-LUMO})/\Delta d_{QD}$ decrease with the increasing polarity of the Si interface bonds, *id est* with increasing charge transfer from the Si core to the interface anions, cf. Fig. 7. For sufficiently polar Si interface bonds, the differences are small. The HOMO-LUMO gap of the GS shows the trend for the absorption gap. As a result, the absorption gaps of small Si QDs embedded in polar dielectrics like SiO_2, Si_3N_4, or metal fluorides (MeF_x) should be smaller and much less dependent on quantum confinement if compared to Si QDs in a weak polar dielectric such as SiC. This effect is depicted in Fig. 3.

Figure 4 shows the HOMO and LUMO energies E_{LUMO}, E_{HOMO} of Si approximants with F, OH, NH_2, CH_3, and H termination, cf. Fig. 1. The energies are shown referring to the vacuum level E_{vac}. The H-terminated Si approximants serve as a reference system due to the nature of the bond Si-H, cf. Sec. III A. Again, E_{HOMO} and E_{LUMO} of the $Si_{35}H_{36}$ and $Si_{35}(OH)_{36}$ approximants are close to the values of Zhou *et al.*[33] Unlike Reboredo and Galli,[37] who obtained unsteady values of E_{HOMO} as a function of the Si core size with CH_3 termination, we observe a steady shift of E_{HOMO} with increasing Si core size of our $Si_x(CH_3)_y$ approximants. The numerical results depicted in Figs. 2, 4, 6, and 7 are supplied in Ref. 48.

Figures 2 and 4 show that there are deviations of the HOMO-LUMO gap and of E_{HOMO}, E_{LUMO} from a monotonic behavior as a function of d_{QD} for approximants which do not possess a very high symmetry ($Si_{14}X_{20}$, $Si_{18}X_{24}$, $Si_{26}X_{32}$, and $Si_{53}X_{48}$, cf. Fig. 1). As will be discussed in Sec. III D, the ratio of Si interface bonds to Si core atoms N_X/N_{Si} has a major influence on the electronic structure of the approximants. For the less symmetric approximants, the ratio N_X/N_{Si} is bigger than for the more symmetric ones, cf. Fig. 8. This results in a small change of the electron transfer over the Si interface bonds to adjacent anions. Consequently, the impact of the symmetry of the Si core on its electronic structure increases with the polarity of the Si interface bonds.

The case of the $Si_{26}X_{32}$ approximants shows another feature which may explain its elevated HOMO-LUMO gap and E_{LUMO}. The Si core has a tetrahedral shape with the T_d symmetry of cubic Si in terms of ⟨111⟩ surfaces with a minimum number of surface bonds, but the numbers of Si atoms in the ⟨001⟩ planes are 2–3–6–4–6–3–2. This "bottleneck" in the Si_{26} core is reflected in an increased localization of the MOs of the Si core, resulting in an increased quantum confinement. In Figs. 2 and 4, the d_{QD} of the high-symmetry Si cores are marked with arrows. If we connect the data points of these approximants, it becomes apparent that the HOMO-LUMO gap as well as E_{HOMO} and E_{LUMO} are a monotonic function of d_{QD}. The symmetry of the Si modifies quantum confinement and thereby the electronic structure.

For the GS, the HOMO and LUMO can be interpreted as the ionization energy E_{ion} and the electron affinity X (Koopman's theorem[57]), respectively.[58] It is worthwhile to note that there are two different values for E_{ion} and X, namely, the atomic and the bulk limits which are shown in Table II for main group IV elements of interest.

Following from the limits in Table II, there must be a transition region for E_{ion} and X. Figures 2 and 4 show that it

TABLE II. Atomic and bulk limit of the electron affinity and ionization energy (Refs. 59 and 60) of Si and germanium (Ge).

	X [eV]		E_{ion} [eV]	
	Atom	Bulk	Atom[a]	Bulk
Si	−1.385	−4.05	8.151	5.17
Ge	−1.244	−4.00	7.898	4.66

[a]First valence electron.

begins around 10 Si atoms (d_{QD}=7.3 Å). For smaller Si cores, a transition to the atomic limit occurs. It scales with the ionicity of bond (IOB) between the interface anion and its neighboring Si atom. This transition can be explained by the ratio of adjacent anion atoms together with a saturation of the charge transfer from the Si core to these anions, resulting in an increase of the HOMO-LUMO gap, cf. Sec. III D. The hybridization of Si atomic orbitals (AOs) at the same energy with a large overlap integral $S_{Si\text{-}Si}$ to a large number of spatially extended MOs is another cause for the shrinking HOMO-LUMO gap with an increasing number of Si atoms. It leads to an energetic and spatial broadening of the discrete single Si hybride AOs and can be described by the Kronig-Penney model.[61]

Depending on the X, E_{ion}, and the electronegativity (EN) of the anions, the approximants experience a significant shift of E_{LUMO}, E_{HOMO}. From Fig. 4 it can be seen that for F-terminated Si cores, E_{LUMO} is shifted down slightly below the Si bulk limit of X. F has the highest values for E_{ion}, X, and EN in the periodic system, cf. Table III. The OMOs and UMOs associated with the F atoms are thus further below the vacuum level E_{vac} than for any other chemical element. The EN of F makes the bond Si-F ionic which results in the F atom controlling the electronic structure of the entire approximant. As a result, X does not approach monotonically to the Si bulk limit, but appears to go through a minimum before it rises again. The values of E_{LUMO} of the $Si_{84}F_{64}$ and $Si_{165}F_{100}$ approximants are −4.554 and −4.541 eV, respectively, which may indicate that the minimum of X is located around d_{QD}=18 Å. Further computations are under way to clarify this point.

An interpretation of the HOMO and LUMO positions depending on the type of interface anions is not straightforward, but we attempt here to deliver a qualitative picture. For strong polar interface bonds, the OMOs are governed by E_{ion} of Si and the interface anion compounded with the electron transfer to the anions expressed by the IOB. With IOB increasing, the E_{ion} of the anions increasingly govern the energetic position of the interface OMOs. If E_{ion} of the interface anions is increasing considerable over E_{ion} of Si and so is the IOB of Si-X, the interface OMOs will be shifted to higher binding energies. This has a "drag-down" effect on the OMOs localized to the Si core as these relax to a higher binding energy, leading eventually to an energetic downshift of the HOMO. This picture is consistent with the average ionization of the Si atoms by interface anions, cf. Fig. 7. Consequently, E_{HOMO} shifts down in energy with increasing IOB and E_{ion} of the interface anion, cf. Fig. 4 and Tables II and III. The UMO position for polar to ionic interface bonds show a similar dependence on X of Si and the interface anions, again with the anions gaining influence with increasing IOB. This results in an energetic shift of the LUMO. However, for covalent or weakly polar interface bonds as for Si_xH_y and $Si_x(CH_3)_y$ approximants, the influence of the interface becomes second to quantum confinement, cf. Fig. 2. The low IOB Si-H and Si-C render the interface to have a minor influence. This results in E_{HOMO} and E_{LUMO} being significantly shifted down and up, respectively, with decreasing size of the approximants.

TABLE III. Electron affinities X, ionization energies E_{ion}, electronegativities EN, and the resulting IOB (Ref. 60) of F, O, N, C, and H to Si.

	X [eV]	E_{ion} [eV][a]	EN[b] ⇝	IOB (X-Si) [%]
F	−3.399	17.42	4.10	75
O	−1.461	13.36	3.50	53
N	+0.07	14.53	3.07	35
C	−1.263	11.26	2.50	13.5
H	−0.756	13.60	2.20	5

[a]First valence electron.
[b]Allred-Rochow; EN (Si)=1.74.

Figure 4 shows that the HOMO energy for a given Si core size beyond the atomic limit follows the sequence F, H, O/C, and N. A similar statement holds for the LUMO energies which follow the sequence F, O, H, C, and N. Due to their low IOB to Si, C and H deviate in these sequences, reflecting the considerations above.

The shift of E_{LUMO} and E_{HOMO} also depends on the ratio of interface anions to the number of Si core atoms (N_{Si}/N_X), cf. Fig. 8. A convergence of E_{HOMO} and E_{LUMO} to the Si bulk limit of $X=E_C$ and $E_{ion}=E_V$ was not observed even for the $Si_{165}F_{100}$ approximants with d_{QD}=18.5 Å. From Fig. 8 we see that the ratio N_X/N_{Si} must be $\ll$0.6 for E_{HOMO}, E_{LUMO} to reach the Si bulk limit. Table III shows the parameters of the anions which have an influence on E_{LUMO} and E_{HOMO}.

In summary, there seem to be three size ranges of Si QDs terminated with anions or functional groups accounting for the respective dielectric matrix. For Si cores with less than 10 Si atoms ($d_{QD}<7$ Å), the atomic limit of E_{ion} and X of both Si and the anion govern the electronic structure exclusively. In an intermediate range which starts around 10 Si atoms ($d_{QD}\approx7.3$ Å), the termination of the Si interface bonds still govern the electronic structure of the Si core, but with departure from the atomic limit. Quantum confinement is evident, but not as pronounced, especially not in the Si cores with a polar or ionic interface termination such as F, OH, and NH_2. The third range is the dominance of the quantum confinement effect due to the Si core HOMO and LUMO determining E_{ion} and X by overcoming the energetic limit given by the anions. We assume that this range starts around $d_{QD}\approx37$ Å, cf. Sec. III D.

C. Density of states for selected approximants

As representative approximants we chose $Si_{35}X_{36}$ (d_{QD} =11 Å). These approximants have an octahedral symmetry

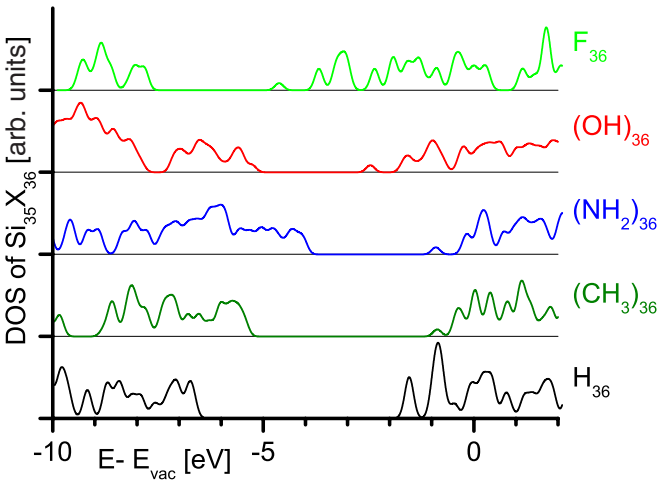

FIG. 5. (Color online) DOS of the $Si_{35}X_{36}$ approximants (d_{QD} =11 Å) as a function of energy and the Si core interface termination.

with a minimum number of Si bonds on the ⟨111⟩ surface planes and are thus energetically favorable, cf. Sec. II B. Figure 5 shows the density of states (DOS) around the HOMO-LUMO gap for these approximants. An artificial broadening of the MOs of 0.1 eV was assumed.

From Fig. 5 we notice that the DOS of approximants with NH_2 and OH terminations are smoother and have less pronounced local extrema compared to approximants with H and F termination and - to a lesser degree - to the approximants with CH_3 termination. Both interface anions, O and N, have an AO symmetry which deviates from that of the Si atoms. Table IV shows the symmetries of the HOMO and LUMO with the corresponding space groups.

The CH_3-terminated approximants show that the symmetry of the Si core can be broken although the interface anion has the same AO symmetry as the Si core due to the shorter bond length Si-C. As a result, the local MO symmetry is altered from cubic (T_d) to trigonal (C_3) by hybridization of the O, N, and C AOs with the MOs of the adjacent atoms of the Si core. This leads to a lifting of MO symmetry constraints. Thereby the degeneracy of Si MOs is broken, yielding a larger number of nondegenerate MOs. The resulting DOS is more continuous with less pronounced local extrema. With an increasing size of the Si core the impact of a lower MO symmetry on the DOS decreases.

D. Charge transfer to the interface

The interface termination of the Si core causes a charge shift to the adjacent anions as a function of the IOB Si-X.

TABLE IV. HOMO and LUMO symmetries of $Si_{35}X_{36}$ approximants with their respective space groups.

X	HOMO	LUMO	Space group
F	T1	A1	T_d
OH	A	A	C_3
NH_2	A	A	C_3
CH_3	A	A	C_3
H	T2	A1	T_d

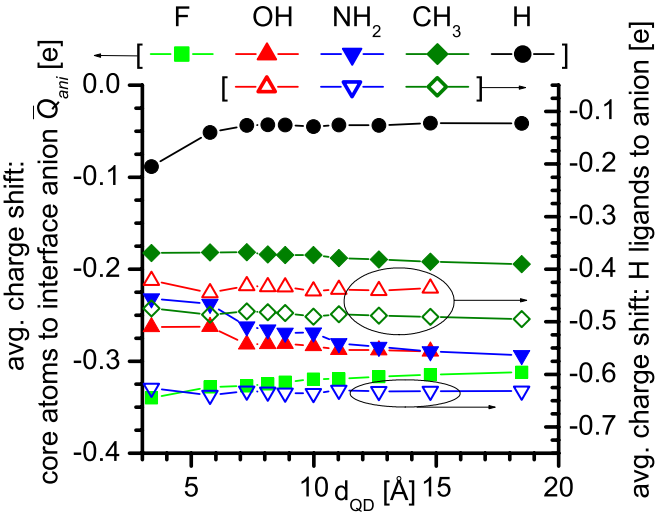

FIG. 6. (Color online) Average charge transfer from the Si core atoms to one interface anion (F, O, N, C, and H: left scale, filled symbols). Average charge transfer from the H ligands to the interface anion of OH, NH_2, and CH_3 groups (right scale, empty symbols).

Figure 6 shows the average charge received by the anions from their H ligands and from the atoms of the Si core.

For approximants with less than 10 Si atoms (d_{QD} <7.3 Å), the charge shift from the Si atoms to the interface anions changes which is consistent with the atomic limit mentioned in Sec. III B. The OH and NH_2 groups show an increase in ionization due to the Coulomb pressure of the Si core decreasing with the number of its ionized Si atoms in compound with the increasing ratio of interface anions to Si atoms N_X/N_{Si}, cf. Figs. 7 and 8. While the former effect increases the ionization of the Si core, the latter one shows that the transferred charge per Si atom has to be shared by an increasing number of interface anions.

The charge transfer from the H ligands to the interface anions only shows a minor change beyond the atomic limit. A change in charge transfer from the H ligands to the interface anions as a function of N_{Si} occurs if the ionization of the interface anions is not compensated by the Si core. There is a small difference in EN between Si and H, rendering the IOB of the bond H-X to be alike to the IOB of the bond Si-X. The value of E_{ion}(H) is bigger than E_{ion}(Si), cf. Tables II and III. This requires more energy for the electron transfer H→X, leading to a deviation of the bond H-X from the bond Si-X. As a consequence, the H ligands are not affected as much as the Si core atoms from the charge transfer to the interface anions, but are ionized to an increasing degree if the interface anion deviates significantly from its charge equilibrium. Exchanging the OH termination of an $Si_{10}(OH)_{16}$ approximant for SiO_2 shows only a marginal change in the electronic structure of the Si core, cf. Sec. III A. The small change in charge transfer H→X as a function of N_{Si} shows that the interface charge transfer from a Si QD to its Si-based dielectric matrix can be approximated reasonably well by the 1-nn approach used in this work.

Figure 6 shows that the behavior of NH_2 terminated Si cores is somewhat different from approximants with other

interface terminations. Beyond the atomic limit the charge transfer to the interface anions slightly increases for CH_3- and OH-terminated approximants as a function of the Si core size. For NH_2-terminated Si cores this increase is more prominent which reveals once more the deviation of N in the row of interface anions investigated. While E_{ion} of N is bigger than E_{ion} of O, the IOB of the bond Si-N and X of N are smaller when compared to Si-O and O, respectively, cf. Table III. With a Si-N IOB of 35%, a significant change in charge transfer is to be expected at a lower Coulomb pressure of the positively charged Si core. An increased charge transfer per anion in the weak ionization regime of the Si core occurs at bigger Si core sizes and is further promoted by the decreasing ratio N_X/N_{Si}.

A further increase in Si core size leads to a saturation limit for the interface charge transfer. This marks the size limit for the interface chemistry as a major impact factor on the electronic structure of Si QDs beyond which E_{LUMO} and E_{HOMO} approach the bulk valence and conduction-band energies of Si.

For H terminated Si approximants, the charge transfer to the H atoms increases to almost twice its value when going from $Si_{10}H_{16}$ to SiH_4. However, the absolute numbers show that there is only a small charge transfer even for SiH_4, so that the Coulomb pressure of the ionized Si atoms does not lead to a saturation in charge transfer. For Si cores with more than 10 atoms, the charge transfer to the H atoms is virtually constant.

The F atoms terminating Si approximants do not have additional H ligands. There is no additional charge compensation counteracting the electron transfer from the Si core. Consequently, the Si core experiences a higher Coulomb pressure to give away its electrons which can be seen in the increase of the negative charge on a high level for the F atoms terminating the Si cores with less than 10 atoms. Moreover, the F termination has a tendency to increase its negative charge monotonically with a shrinking size of the Si core, which can be attributed to its extremely high values for the EN, X, and E_{ion}.

The ratio N_X/N_{Si} has a hyperbolic dependence on N_{Si} due to the quotient of surface area and volume of the Si core. This can be seen at the average charge transfer for one Si atom to the interface anions X, cf. Fig. 7.

Empirical fitting to N_X/N_{Si} of the approximants of this work yielded

$$[N_X/N_{Si}]_{fit} = 1.866 \times \frac{6}{d_{Si}[\text{Å}]}. \quad (1)$$

A closer examination of Si cores of high symmetry with the constraint of having ⟨111⟩ surfaces only (octahedral shape) reveals that we can obtain their number of Si atoms by the geometrical series

$$N_{Si}[i] = N_{Si}[i-1] + (2i+1)^2 \quad \forall\, i \geq 0. \quad (2)$$

The number of interface bonds for these Si cores can be determined by

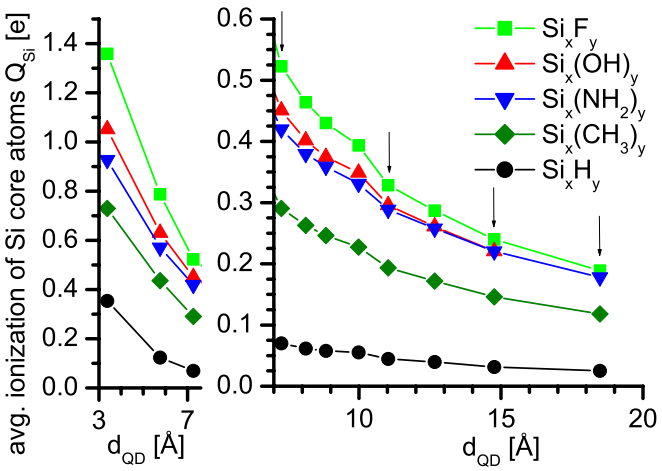

FIG. 7. (Color online) Average ionization of Si core atoms by interface anions (F, O, N, C, and H). For clarity, the graph is split into two subgraphs with different charge scale. Both graphs show the points for the $Si_{10}X_{16}$ approximants (d_{QD}=7.3 Å). Arrows indicate the high-symmetry approximants $Si_{10}X_{16}$, $Si_{35}X_{36}$, $Si_{84}X_{64}$, and $Si_{165}X_{100}$.

$$N_X[i] = N_X[i-1] + (8i+4) \quad \forall\, i \geq 0$$
$$= 4(i+1)^2. \quad (3)$$

The SiX_4, $Si_{10}X_{16}$, $Si_{35}X_{36}$, $Si_{84}X_{64}$, and $Si_{165}X_{100}$ approximants investigated in this work belong to this group of high-symmetry approximants, cf. Fig. 1. The ratio N_X/N_{Si} of approximants with octahedral shape and ⟨111⟩ surfaces together with the fit of Eq. (1) is shown in Fig. 8.

Even for large N_{Si} the ratio N_X/N_{Si} is not significantly smaller. Judging from the HOMO and LUMO energies and N_X/N_{Si} of the approximants, we propose that the interface to

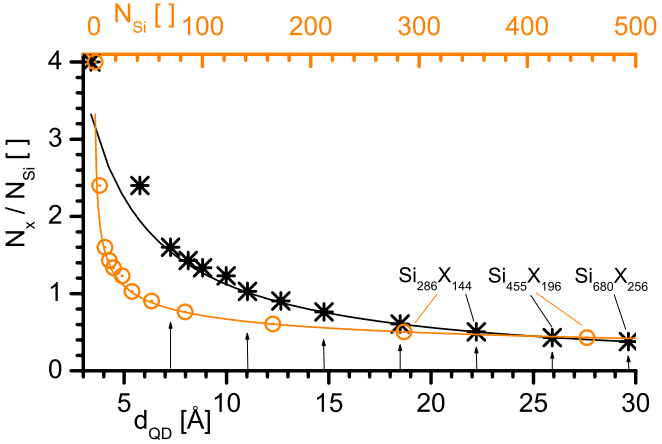

FIG. 8. (Color online) Ratio of the interface anions/functional groups X to Si core atoms as a function of d_{QD} (black) and as a function of the number of Si core atoms (orange/gray). The points present the approximants computed in this work and the next biggest high-symmetry approximants beyond $Si_{165}X_{100}$ derived from Eqs. (2) and (3). The lines present results from the fit [Eq. (1)]. Arrows indicate high-symmetry approximants, see also text and Figs. 2 and 4.

a polar dielectric has a major influence on the electronic structure down to a ratio of $N_X/N_{Si} \approx 0.3$. The values for $i=9$ suggest that Si QDs with $d_{QD} \leq 37.1$ Å or ≤ 1330 Si atoms embedded into SiO_2 or Si_3N_4 have an electronic structure which is controlled significantly by the dielectric. This value can be considered as a minimum, because the high-symmetry approximants have the lowest ratio N_X/N_{Si} for a $\langle 111 \rangle$ terminated Si nanocrystal of a given number of Si atoms N_{Si}. For corroborating this statement, a $Si_{525}H_{276}$ approximant computed by Öğüt *et al.*[62] yields $d_{QD}=27.2$ Å and $N_X/N_{Si}=0.526$. The high-symmetry approximants with the nearest numbers of Si atoms are $Si_{455}X_{196}$ ($d_{QD}=25.9$ Å) and $Si_{680}X_{256}$ ($d_{QD}=29.6$ Å), yielding $N_X/N_{Si}=0.431$ and $N_X/N_{Si}=0.376$, respectively.

IV. CONCLUSION

We investigated Si core approximants by DF-HF ground-state calculations within the B3LYP hybride functional formalism and a 6–31G(d) Gaussian type MO basis set. The Si cores were fully terminated with F, OH, NH_2, CH_3, and H, accounting for metal fluoride, SiO_2, Si_3N_4, and SiC matrices. The Si_xF_y and Si_xH_y approximants served as model systems for an ionic and covalent interface. The spherical Si cores are terminated by $\langle 111 \rangle$ planes and comprise of 1–165 atoms which corresponds to a QD diameter of $d_{QD}=3.4$–18.5 Å.

We found three ranges for the electronic structure of Si cores. The atomic limit applies to Si cores with a diameter <7 Å (10 Si atoms). A transition range comprises Si cores with a diameter from 7 to ≈ 37 Å (ca. 1330 Si atoms), where the interface has a significant impact on the electronic structure for strong polar or ionic interfaces (F, OH, and NH_2). The bulk limit governs the electronic structure for Si cores beyond ca. 37 Å diameter, whereby the influence of quantum confinement is still important for weakly polar or covalent interfaces (CH_3 and H).

For highly polar Si interface bonds, the nature of the interface governs the electronic structure, thereby reducing the impact of quantum confinement. This results in the HOMO-LUMO gap not changing significantly over a rather wide size range of the Si core. Our findings do not deliver a confirmation of results from the literature after which a diminished band gap is primarily caused by atomic displacement of Si atoms experienced by the surrounding dielectric matrix.[51] We noticed only a minor impact of interface stress on the HOMO-LUMO gap, whereby the local deviation from the MO symmetry of the Si core as a function of the interface anion has a significant influence. A deconvolution of both phenomena regarding the impact on the HOMO-LUMO gap is another complex issue which still has to be explored in more detail. Due to the interface impact the HOMO energy depends on the ionization energies of Si and the anions along with the ionicity of the interface bonds, while the LUMO energy shows the same dependence on the ionicity of bond with the respective electron affinity as boundary condition. The ratio of interface anions to Si core atoms N_X/N_{Si} plays a decisive role in the electronic structure as shown by the ionization rate of the Si core atoms. We introduced a general description of any sum formula of high-symmetry Si core approximants of octagonal shape with $\langle 111 \rangle$ Si surface planes by utilizing geometrical series. These sum formulas give an estimate of the ratio N_X/N_{Si} for any approximant with the geometric constraints mentioned.

The spatial symmetry of the Si cores has an increasing influence on the electronic structure with an increasing ionicity of bond to the interface anions. Different MO symmetries of polar functional groups with H ligands cause a local breakdown of MO symmetry, leading to a lifting of the MO degeneracy of the Si core and a more continuous DOS with less pronounced local extrema.

ACKNOWLEDGMENTS

The authors wish to acknowledge the financial support by the Australian Research Council (ARC) Centre of Excellence funding scheme and financial support by the Global Energy Climate Project (GCEP). D. König is very thankful to R. Scholz, Walter Schottky Institut, TU München, 85748 Garching, Germany, and S. Gemming, Institut für Ionenstrahlphysik & Materialforschung, Forschungszentrum Rossendorf, 01328 Dresden, Germany, for numerous discussions during his Ph.D. years at the Institute of Physics, TU Chemnitz, Germany.

*dirk.koenig@unsw.edu.au; http://www.pv.unsw.edu.au/

[1] C. Langer, R. Ozeri, J. D. Jost, J. Chiaverini, B. DeMarco, A. Ben-Kish, R. B. Blakestad, J. Britton, D. B. Hume, W. M. Itano, D. Leibfried, R. Reichle, T. Rosenband, T. Schaetz, P. O. Schmidt, and D. J. Wineland, Phys. Rev. Lett. **95**, 060502 (2005).

[2] D. Schrader, I. Dotsenko, M. Khudaverdyan, Y. Miroshnychenko, A. Rauschenbeutel, and D. Meschede, Phys. Rev. Lett. **93**, 150501 (2004).

[3] L. V. Asryan and S. Luryi, Solid-State Electron. **47**, 205 (2003).

[4] G. Chen, R. Rapaport, D. T. Fuchs, L. Lucas, A. J. Lovinger, S. Vilan, A. Aharoni, and U. Banin, Appl. Phys. Lett. **87**, 251108 (2005).

[5] M. A. Green, Prog. Photovoltaics **9**, 123 (2001).

[6] A. J. Nozik, Physica E (Amsterdam) **14**, 115 (2002).

[7] M. A. Green, *Third Generation Solar Cells* (Springer, New York, 2003).

[8] Australian Research Council Photovoltaics Centre of Excellence Annual Reports 2002–2006 (unpublished); http://www.pv.uns.edu.au/annualreports.asp.

[9] General Climate Energy Project (GCEP), http://gcep.stanford.edu/pdfs/QeJ5maLQQrugiSYMF3ATDA/2.2.6.green_06.pdf.

[10] N.-M. Park, T.-S. Kim, and S.-J. Park, Appl. Phys. Lett. **78**, 2575 (2001).

[11] P. Würfel, Sol. Energy Mater. Sol. Cells **46**, 43 (1997).

[12] P. Würfel, *The Physics of Solar Cells: From Principles to New Concepts* (Wiley, New York, 2005).
[13] R. T. Ross and A. Nozik, J. Appl. Phys. **53**, 3813 (1982).
[14] N. J. Ekins-Daukes, K. W. J. Barnham, J. P. Connolly, J. S. Roberts, J. C. Clark, G. Hill, and M. Mazzer, Appl. Phys. Lett. **75**, 4195 (1999).
[15] M. Mazzer, K. W. J. Barnham, I. M. Ballard, A. Bessiere, A. Ionannides, D. C. Johnson, M. C. Lynch, T. N. D. Tibbits, J. S. Roberts, G. Hill, and C. Calder, Thin Solid Films **511-512**, 76 (2006).
[16] H. Takagi, H. Ogawa, Y. Yamazaki, A. Ishizaki, and T. Nakagiri, Appl. Phys. Lett. **56**, 2379 (1990).
[17] V. Ranjan, V. A. Singh, and G. C. John, Phys. Rev. B **58**, 1158 (1998).
[18] F. Iacona, G. Franzò, and C. Spinella, J. Appl. Phys. **87**, 1295 (2000).
[19] G. H. Li, K. Ding, H. X. Han, and Z. P. Wang, J. Appl. Phys. **88**, 1439 (2000).
[20] G. Ledoux, J. Gong, F. Huisken, O. Guillois, and C. Renaud, Appl. Phys. Lett. **80**, 4834 (2002).
[21] L. Ding, T. P. Chen, Y. Liu, M. Yang, and J. I. Wong, J. Appl. Phys. **101**, 103525 (2007).
[22] M. V. Wolkin, J. Jorne, P. M. Fauchet, G. Allan, and C. Delerue, Phys. Rev. Lett. **82**, 197 (1999).
[23] X. X. Wang, J. G. Zhang, L. Ding, B. W. Cheng, W. K. Ge, J. Z. Yu, and Q. M. Wang, Phys. Rev. B **72**, 195313 (2005).
[24] T. V. Torchynska, J. Non-Cryst. Solids **352**, 2484 (2006).
[25] A. Zimina, S. Eisebitt, W. Eberhardt, J. Heitmann, and M. Zacharias, Appl. Phys. Lett. **88**, 163103 (2006).
[26] J. Knipping, H. Wiggers, B. Rellinghaus, P. Roth, D. Knojhodzic, and C. Meier, J. Nanosci. Nanotechnol. **4**, 1039 (2004).
[27] C. Meier, A. Gondorf, S. Lüttjohann, A. Lorke, and H. Wiggers, J. Appl. Phys. **101**, 103112 (2007).
[28] I. Vasiliev, J. R. Chelikowsky, and R. M. Martin, Phys. Rev. B **65**, 121302(R) (2002).
[29] A. Puzder, A. J. Williamson, J. C. Grossman, and G. Galli, Phys. Rev. Lett. **88**, 097401 (2002).
[30] M. Luppi and S. Ossicini, J. Appl. Phys. **94**, 2130 (2003).
[31] M. Luppi and S. Ossicini, Phys. Rev. B **71**, 035340 (2005).
[32] A. B. Filonov, S. Ossicini, F. Bassani, and F. Arnaud d'Avitaya, Phys. Rev. B **65**, 195317 (2002).
[33] Z. Zhou, L. Brus, and R. Friesner, Nano Lett. **3**, 163 (2003).
[34] L. E. Ramos, J. Furthmüller, and F. Bechstedt, Phys. Rev. B **70**, 033311 (2004).
[35] M. Wang, D. Li, Z. Yuan, D. Yang, and D. Que, Appl. Phys. Lett. **90**, 131903 (2007).
[36] L. Dal Negro, J. H. Yi, L. C. Kimerling, S. Hamel, A. Williamson, and G. Galli, Appl. Phys. Lett. **88**, 183103 (2006).
[37] F. Reboredo and G. Galli, J. Phys. Chem. B **109**, 1072 (2005).
[38] M. Zacharias, L. Tsybeskov, K. D. Hirschmann, P. M. Fauchet, J. Bläsing, P. Kohler, and P. Veit, J. Non-Cryst. Solids **227-230**, 1132 (1998).
[39] M. Zacharias, J. Heitmann, R. Scholz, U. Kahler, M. Schmidt, and J. Bläsing, Appl. Phys. Lett. **80**, 661 (2002).
[40] R. L. Ligenza, J. Phys. Chem. **65**, 2011 (1961).
[41] D. J. Eaglesham, A. E. White, L. C. Feldman, N. Moriya, and D. C. Jacobson, Phys. Rev. Lett. **70**, 1643 (1993).
[42] M. J. Frisch *et al.*, GAUSSIAN03, Revision D 0.1, Gaussian, Inc., Wallingford, CT, 2004.
[43] R. Dennington II, *et al.*, GAUSSVIEW, version 3.09, Semichem, Inc., Shawnee Mission, KS, 2003.
[44] A. D. Becke, Phys. Rev. A **38**, 3098 (1988).
[45] C. Lee, W. Yang, and R. G. Parr, Phys. Rev. B **37**, 785 (1988).
[46] J. B. Foresman and Æ. Frisch, *Exploring Chemistry with Electronic Structure Methods* (Gaussian., Pittsburgh, PA, 1996), Chap. 7.
[47] L. A. Curtiss, K. Raghavachari, and J. A. Pople, J. Phys. Chem. **98**, 1293 (1993).
[48] See EPAPS Document No. E-PRBMDO-78-101827 for a critical discussion of the computational accuracy and numeric values of the computations carried out. For more information on EPAPS, see http://www.aip.org/pubservs/epaps.html.
[49] D. König *et al.* (unpublished).
[50] C. S. Garoufalis and A. D. Zdetsis, Phys. Chem. Chem. Phys. **8**, 808 (2006).
[51] G. Hadjisavvas and P. C. Kelires, Physica E (Amsterdam) **38**, 99 (2007).
[52] E. H. Nicollian and J. R. Brews, *MOS (Metal Oxide Semiconducote) Physics and Technology* (Wiley, New York, 1982), p. 41.
[53] F. Bart, M. Gautier, F. Jollet, and J. P. Duraud, Surf. Sci. **306**, 342 (1994).
[54] H. A. Jahn and E. Teller, Proc. R. Soc. London, Ser. A **161**, 220 (1937).
[55] J. P. Perdew, K. Burke, and M. Ernzerhof, Phys. Rev. Lett. **77**, 3865 (1996).
[56] M.-S. Yang, K.-S. Cho, J.-H. Jhe, S.-Y. Seo, and J. H. Shin, Appl. Phys. Lett. **85**, 3408 (2004).
[57] T. Koopmans, Physica (Amsterdam) **1**, 104 (1934).
[58] R. G. Parr and W. Wang, *Density-Functional Theory of Atoms and Molecules* (Oxford University Press, New York, 1989).
[59] K. W. Böer, *Survey of Semiconductor Physics* (Van Nostrand Reinhold, New York, 1992), Vol. I.
[60] A. F. Holleman and N. Wiberg, *Lehrbuch der Anorganischen Chemie*, 101st ed. (de Gruyter, Berlin, 1995).
[61] J. H. Davies, *The Physics of Low-Dimensional Semiconductors: An Introduction* (Cambridge University Press, New York, 1998), p. 177.
[62] S. Öğüt, J. R. Chelikowsky, and S. G. Louie, Phys. Rev. Lett. **79**, 1770 (1997).